Journal of Magnetic Resonance 205 (2010) 209–215

Contents lists available at ScienceDirect

Journal of Magnetic Resonance

journal homepage: www.elsevier.com/locate/jmr

Propagator-resolved 2D exchange in porous media in the inhomogeneous magnetic field

Lauren M. Burcaw, Mark W. Hunter, Paul T. Callaghan *

MacDiarmid Institute for Advanced Materials and Nanotechnology, School of Chemical and Physical Sciences, Victoria University of Wellington, Wellington 6001, New Zealand

ARTICLE INFO

Article history:
Received 24 February 2010
Revised 13 April 2010
Available online 6 May 2010

Keywords:
Porous media
Diffusion
Exchange
Inhomogeneous fields
Susceptibility

ABSTRACT

We present a propagator-resolved 2D exchange spectroscopy technique for observing fluid motion in a porous medium. The susceptibility difference between the matrix and the fluid is exploited to produce an inhomogeneous internal magnetic field, causing the Larmor frequency to change as molecules migrate. We test our method using a randomly packed monodisperse 100 μm diameter glass bead matrix saturated with distilled water. Building upon previous 2D exchange spectroscopy work we add a displacement dimension which allows us to obtain 2D exchange spectra that are defined by both mixing time and spatial displacement rather than by mixing time alone. We also simulate our system using a Monte Carlo process in a random nonpenetrating monodisperse bead pack, finding good agreement with experiment. A simple analytic model is used to interpret the NMR data in terms of a characteristic length scale over which molecules must diffuse to sample the inhomogeneous field distribution.

1. Introduction

The diffusion of molecules imbibed in a porous medium has relevance to biology, petrophysics, and chemical engineering. In particular, the measurement of time-dependent diffusion can provide information about the structure of the system being studied. NMR presents a number of noninvasive approaches to such measurement. Pulsed Gradient Spin Echo (PGSE) NMR [1] allows one to measure the diffusion of spins by applying stepped magnetic field gradient pulses and noting the echo attenuation caused by dephasing. Such PGSE NMR methods allow one to measure specific translational displacements over a well-defined displacement time. We describe here a new experiment in which such measured displacements of spin-bearing molecules are correlated with changes in local magnetic field.

Before detailing our method we briefly review some prior methodology. Spin-echo measurements of relaxation have proven an alternative route to studying diffusion. Pore surfaces influence relaxation so that molecules resident in small pores, with large surface to volume ratios, have shorter relaxation times. Consequently, the rate of T_2 relaxation is related to the pore size distribution of a porous system [2], and therefore in an exchange experiment, any changes in T_2 will provide evidence for inter-pore migration. A 2D T_2 exchange method has been proposed to track the pore to pore movement of fluid through a porous system [3,4]. These methods rely on the 2D inverse Laplace transform [5] which results in pearling effects [6], which generate distinct off-diagonal peaks. The growth of these off-diagonal peaks in the 2D relaxation spectrum and can be interpreted as arising from diffusion between pores of different sizes. Finally, susceptibility inhomogeneity between the matrix and the pore space leads to inhomogeneous local magnetic fields when the porous medium is placed in the magnet used for NMR measurements. Diffusion of molecules in these inhomogeneous internal fields results in dephasing of the spins and a consequent spin echo decay. Dephasing due to diffusion in the internal field (DDIF) can also be used to study the pore geometry in rocks [7]. By increasing the time water is allowed to diffuse through a pore space with a highly inhomogeneous field, one can find where the spin echo DDIF approaches zero to define a characteristic time that can be used as a direct measure of the pore space. Such pore to pore fluid transfer can also be studied by using 2D exchange methods, which measure the NMR magnetization at two different times, resulting in two different NMR spectra [8].

In a previous paper [9] we demonstrated a 2D exchange technique to investigate molecular motion through a porous media in an inhomogeneous magnetic field. We explored the molecular motion of water molecules through two sizes of monodisperse glass bead packs. To do this we used a two-dimensional pulse sequence similar to a NOESY [10] with a frequency encoding and acquisition time separated by a mixing time, τ_m which would allow the water molecules time to diffuse through the pore system. We took a Fourier transform of the raw data to produce a 2D spectrum. An inhomogeneous magnetic field exists in this pore system due to the susceptibility differences between the water and the glass beads which causes a broadening in the 1D spectrum [11,12]. As water

* Corresponding author. Fax: +64 6 350 5164.
E-mail address: Paul.Callaghan@vuw.ac.nz (P.T. Callaghan).

1090-7807/$ - see front matter © 2010 Elsevier Inc. All rights reserved.
doi:10.1016/j.jmr.2010.04.020

molecules diffuse through the inhomogeneous magnetic field, they cause a broadening in the off-diagonal width of the 2D spectra. As the mixing time is increased, the mean diffusion distance increases, resulting in an increasing off-diagonal intensity.

A limitation of both the T_2 exchange experiment and the inhomogeneous local field exchange experiment is that only temporal insight is obtained. For example, the T_2 exchange experiment cannot distinguish between signals originating from molecules that have remained within their starting pore and molecules that have diffused from a starting pore to a similarly sized pore. To differentiate between these signals, Washburn and Callaghan introduced an additional displacement dimension by inserting a third encoding parameter, the response of the spectrum to a PGSE gradient pulse pair. On Fourier transformation with respect to this dimensions, a displacement propagator results, giving probabilities of displacement along the direction of the applied magnetic field gradient pulse [13,14]. By adding the displacement dimension, Washburn and Callaghan were able to select planes of T_2 exchange spectra separated by displacement, and for different values of the mixing time allowed for exchange.

In this article we report on a similar extension of the inhomogeneous local field exchange experiment in which a third displacement dimension is included. In the earlier 2D version of the experiment, the off-diagonal intensity arises from all molecules which have changed their local field value, irrespective of the distance travelled. By including the propagator dimension we are now able to distinguish molecules which have diffused different distances along the field gradient axis. Hence, rather than measuring an off-diagonal intensity which is a function of mixing time alone, we add a displacement dimension, allowing a spatio-temporal analysis of the diffusion between sites of differing field. Of course the connection between space and time, in this context, is provided by the diffusion rate, and the characteristic length scale over which local fields change significantly, as measured by the spread of Larmor frequencies in the NMR spectrum. The ability to access the spatial information therefore provides a more robust check on any model used to interpret our experimental results. It is this use of a well-defined spatial dimension which differentiates our method from earlier local field exchange methods such as DDIF or the 2D method described in reference [9].

The new data we acquire consist of two-dimensional spectra where axes are labeled by the frequency spread corresponding to the inhomogeneous field. We then focus our attention to the off-diagonal intensity of these spectra at some particular frequency offset. This is done to establish the degree of exchange that is occurring during the mixing period. We then measure the intensity as a function of molecular displacement, Z, and mixing time, τ_m, using the label $I(Z,\tau_m)$. We adopt two approaches in the interpretation of our data. First, we model the internal fields in a random bead pack and simulate the restricted diffusive motion of molecules within that pack, thus gaining estimates of $I(Z,\tau_m)$. Second, we adopt a simple analytic model for the migration of NMR signal away from the spectral diagonal by assuming an isotropic Gaussian propagator with effective diffusion coefficient D_{eff}, and a measure of the degree of randomizing of the NMR frequency within the inhomogeneous field spectrum which depends on total displacement R as $1-\exp(-R^2/2l_c^2)$, where l_c is some characteristic length scale.

While our new method has strong links with prior work, such as DDIF and T_2-exchange methods, it is distinct in a number of regards. First it is "many-dimensional", having both evolution and acquisition frequency domains, f_1 and f_2, a mixing time dimension, and a displacement dimension. Second, the use of pulsed field gradient encoding allows direct determination of molecular displacements, rather than via an indirect deduction based on a known diffusion time and an assumed effective diffusion coefficient, as implied in DDIF. Finally, the multitude of dimensions allows for different modes of analysis, by selecting different "planes" of parameters, or, as we shall show, by comparing with model predictions, we produce a two-dimensional surface, rather than a one-dimensional graph.

2. Method

2.1. Experimental

All experiments were performed at 22 °C on a 400 MHz Bruker spectrometer using the proton signal from distilled water in a random dense pack of monodisperse glass spheres. The glass beads are comprised of soda lime glass of mean diameter 97.6 μm with a standard deviation of 3.6 μm (Duke Scientific Products, Fremont, CA).

2.1.1. Pulse sequence

The pulse sequence used is shown in Fig. 1. To prevent interaction between the applied gradients and the internal magnetic field gradients of the sample [15], we use bipolar pulsed field gradients of strength g with a storage time Δ measured between the beginnings of each gradient pair. For each n, we step the applied gradients p times to a maximum strength of 13.5 G cm^{-1} and incrementally increase the frequency encoding time, t_1 by a increment equal to 1/bandwidth, in our case (20 kHz)$^{-1}$ or 50 μs. Since we want to keep the storage time Δ constant for all n, we include a spin echo sequence before the diffusion measurement to allow us to increment t_1. Note that the spin echo produced from this spin echo sequence will appear at a time t_1 after the 180°. The time between the first and second 180° is 1.01 ms. Due to the broadened 1D spectrum, half the signal from this echo will have decayed at a t_1 of 192 μs. Thus we will only forfeit a small amount of resolution in our final 2D spectrum. After the first applied gradient pair, a 90° pulse stores the magnetization along the z axis to eliminate any effect from T_2 relaxation, however, the protons still undergo

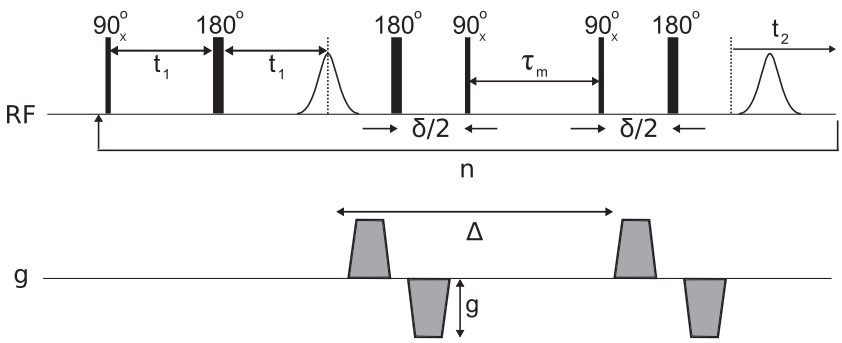

Fig. 1. Pulsed sequence used for the propagator-resolved field exchange experiment.

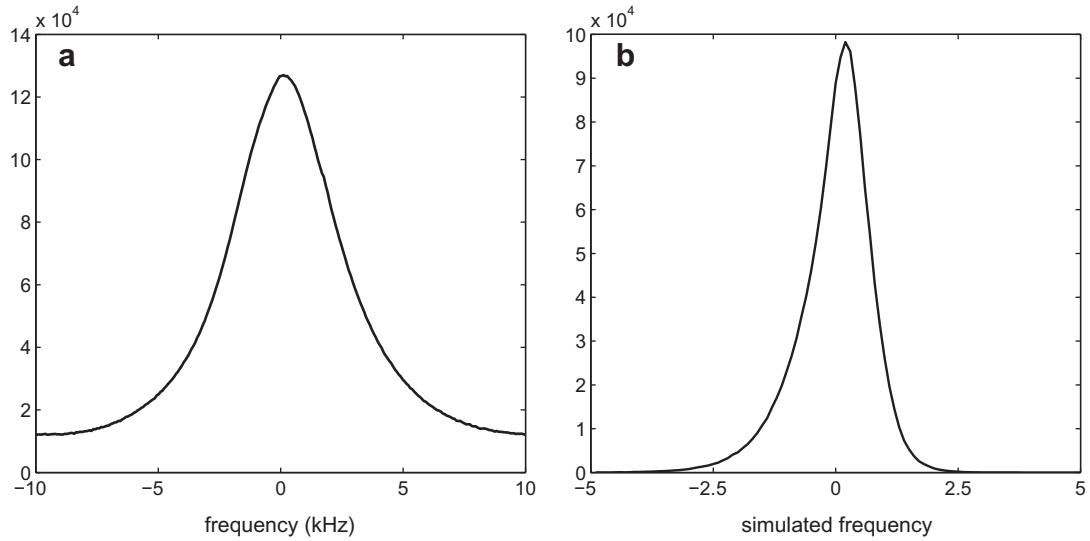

Fig. 2. (a) The measured 1D ^{1}H NMR spectrum for the water in glass bead pack at 400 MHz. The spectrum has an FWHM of 5.2 kHz. (b) The simulated NMR spectrum for a random bead pack. Frequency units are dimensionless and the spectrum has an FWHM of 1.1.

T_1 relaxation. After a mixing time, τ_m, which is approximately Δ, the magnetization is brought back to the transverse plane and the second pair of gradients are pulsed to complete the diffusion measurement. We acquire for a time t_2 following a time δ after the final 90° pulse. To ensure the resultant signal is only that derived from the initial 90° pulse, we utilize a 16 step phase cycling.

This pulse sequence produces an $m \times n \times p$ data matrix where m is the number of acquisition points, n the number of time evolution steps and p the number of q-gradient steps. For all experiments we acquire for 128 points (acquisition time 6.4 ms), increment t_1 64 times (evolution time 3.3 ms) and step our applied gradients 33 times for a data matrix of size $128 \times 64 \times 33$ which we zero fill to $256 \times 256 \times 64$ and apply a 3D fast Fourier transform. All data is processed using Matlab (MathWorks, Natick, MA).

The one-dimensional NMR spectrum for the water/beadpack sample is shown in Fig. 2a.

2.2. Simulations

We have built upon a computer model created by Hunter et al. [16] which generates a random bead pack and uses a random walk model to simulate diffusion throughout its pore space. To create the bead pack we drop spheres one by one into a cylinder of diameter 10 bead diameters and allow the beads to reach their potential energy minimum. For our simulation, we use 792 beads with a height of approximately 10 bead diameters. Our calculated porosity is 39.3%.

The modeling of diffusion is based on a random-walk model where tracers step a length r per time step t where the step length is defined by

$$r(t + \Delta t) = r(t) + \sqrt{2D_0}\Delta W(t) \quad (1)$$

where D_0 is the self diffusion coefficient, and $\Delta W(t)$ is a Gaussian random variable with variance Δt. During this diffusion process, the sphere pack is treated as gridded spheres of diameter 10 units. If a tracer encounters a sphere at the end of any step, that step is rejected and retried until it ends without encountering a sphere. We allow the tracers to diffuse for specified times which match our experimental storage times and obtain final tracer position data.

To generate the internal field, we treat each sphere as a magnetic dipole oriented at the sphere center in the z-direction and take the magnetic field at each mesh cube as a superposition of the magnetic field from all spheres in the bead pack.

However, to eliminate the possibility of tracers diffusing outside of the observation area, we select a cube of size 4.5 bead diameters per side centered in the middle of the cylinder and break it into a $120 \times 120 \times 120$ mesh of size 0.075 bead diameters, and include in our processing only those tracers which originate inside this cube.

The resultant internal field is shown in Fig. 3 which shows an xz slice of the center of our model cube with a much smaller mesh size of 0.0187 bead diameters to better display the internal magnetic field.

For each simulated storage time, we determine the displacement and recalculate the internal magnetic field offset based on the final positions of the tracers.

Relative to each bead, one can see that the field tends to be strongest (light) at the z-direction poles, and lowest (dark) at the equators. While the 1D spectrum shown in Fig. 2b shows a positive skew, however the average of this spectrum is slightly negative at −0.0191. This skew is probably due to edge effects caused by our finite sized bead pack.

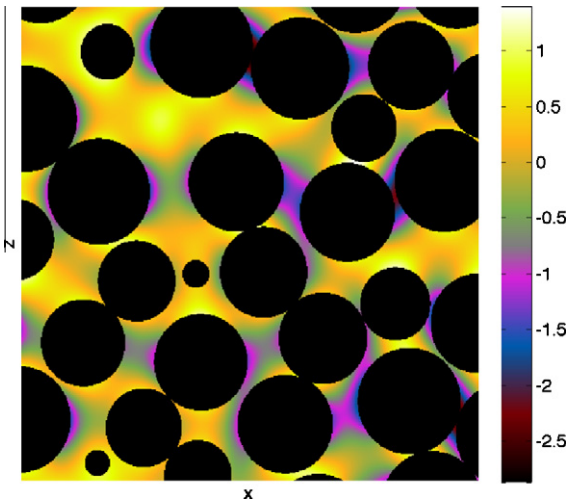

Fig. 3. The simulated internal magnetic field for the center y slice of the volume investigated where all spheres in the pack contribute to the field calculation. The internal magnetic field is in dimensionless units.

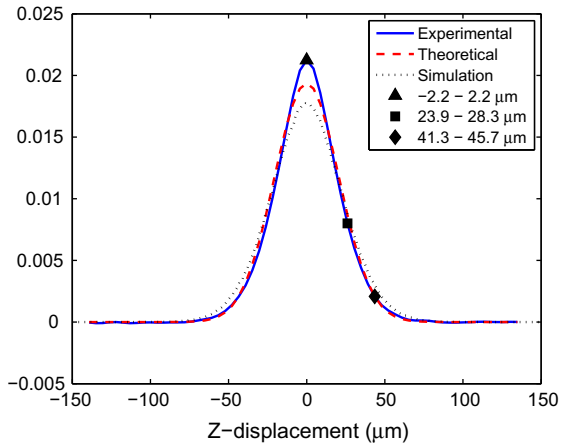

Fig. 4. Propagator for a mixing time of 160 ms. The experimental data is shown by the solid line. The calculated theoretical propagator as given by Eq. (3) using an effective diffusion of $0.65D_0$ is shown by the dashed line. The simulated propagator is shown by the dotted line. The markers ▲, ■, and ♦ indicate Z-displacements of −2.2 to 2.2 μm, 21.7–30.5 μm, and 41.3–45.7 μm, respectively. The experimental and theoretical propagators have a resolution of about 8.7 μm, but the echo attenuations are zero filled to 64 points before Fourier transformation.

3. Experimental and simulation results

Fig. 4 shows the Z-displacement propagator for a mixing time of 160 ms. This corresponds to a Δ of 162 ms. The experimentally measured propagator is shown by the solid line and has a resolution of 3.5 μm. For molecules diffusing in a random pore glass with pore separation b, the expected echo attenuation is the diffusive–diffraction behavior, as given in the pore hopping model [17] by

$$E(q,\Delta) = |S_0(q)|^2 \exp\left(-\frac{6D_{eff}\Delta}{b^2}\left[1-\frac{\sin(qb)}{qb}\right]\right) \quad (2)$$

where $|S_0(q)|^2$ is the pore structure factor and the q vector magnitude is $\gamma\delta g$. For asymptotic conditions, $D_{eff}\Delta \gg b^2$, this expression reduces to $\exp(-q^2 D_{eff}\Delta)$ for which the asymptotic propagator is given by the Gaussian

$$P(Z,\Delta) = (4\pi D_{eff}\Delta)^{-1/2} \exp\left(-\frac{Z^2}{4D_{eff}\Delta}\right) \quad (3)$$

where Z represents displacements along the gradient axis. Given Δ = 162 ms, and fitting to the low q^2 limit of the echo attenuation $E(q)$ (i.e. from the mean-squared displacement $D_{eff} = \langle Z^2\rangle/2\Delta$), we find an effective diffusion of $D_{eff} = 0.65D_0$ where D_0 is the diffusion coefficient of bulk water. The theoretical propagator is shown by the dashed line and agrees moderately well with experiment. The slightly different experimental propagator shape probably arises because the asymptotic conditions for diffusion have not quite been reached at 160 ms, and therefore the actual propagator is not yet gaussian. The dotted line is the propagator found by simulation at a mixing time of 160 ms. Again, to determine an effective diffusion coefficient, we derive $E(q)$ from the simulated propagator and fit for q^2 in the low q limit. For the simulations, the effective diffusion coefficient at 162 ms is found to be $0.74D_0$ where D_0 is the bulk diffusion constant.

Fig. 5 shows the approach to asymptotic conditions as the mixing time is increased of D_{eff} for both experiment and simulations. For both the experiments and simulation, asymptotic conditions have not been fully reached at 640 ms, however the limit is sufficiently close that a reasonable estimate can be made for the purpose of calculating porosity. In a bead pack the expected asymptotic diffusion coefficient is $\sqrt{\phi}D_0$ where ϕ is the porosity [18]. For the experiments, where we find ϕ = 0.436, this agrees well with this expected limit. The simulated bead pack has a porosity of 0.393, suggesting an asymptotic D_{eff} of $0.63D_0$. This estimate is consistent with Fig. 5, and suggests that asymptotic conditions have not yet been reached at 162 ms in the case of the simulations. It is possible that choice of a sampling cube of side length 4.5 bead diameters may have been insufficient to obtain a representative elementary volume. In fact, we find the average of the B_z field in Fig. 2b to be −0.0191 suggesting we do not have full anisotropy in the cube. We are constrained by computer memory with regards to the size of this cube, however the simulations presented do provide a useful comparison.

We can select 2D spectra along the propagator dimension which correspond to spectra containing the NMR signals from molecules which have diffused a specific range of Z-displacements. The top row of Fig. 6 shows the experimental spectra obtained at

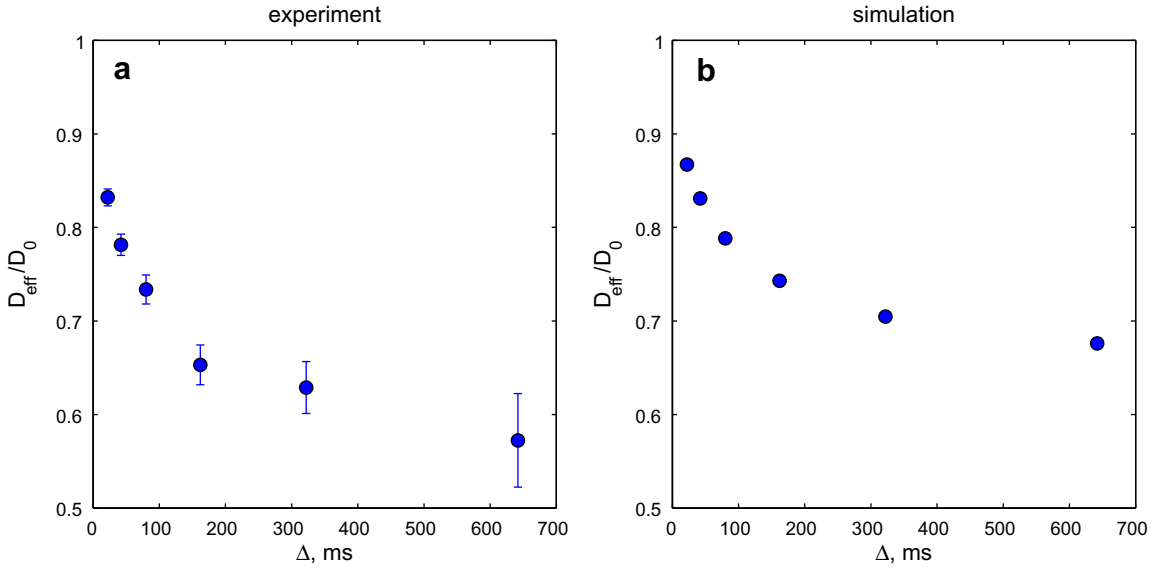

Fig. 5. (a) The ratio of effective diffusion to bulk diffusion for a 100 μm beadpack from experiment using the pulse sequence shown in Fig. 1 using a maximum gradient of 5 G/mm and without t_1 stepping. (b) The ratio of effective diffusion to bulk diffusion for the simulation. Note error bars are inside the markers.

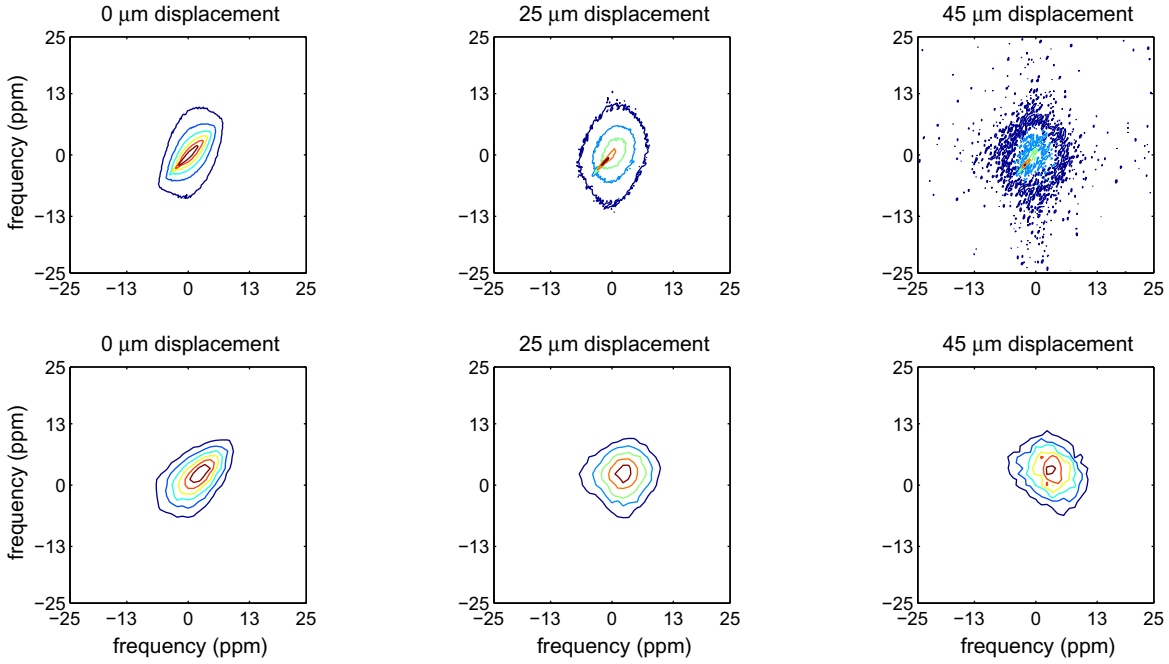

Fig. 6. 2D spectra for a τ_m of 160 ms. Top row: obtained using experimental data. Bottom row: obtained using simulated data.

τ_m = 160 ms for Z-displacements of 0 μm, 25 μm, and 45 μm which correspond to the markers ▲, ■, and ♦ on the experimental propagator in Fig. 4.

Since a molecule diffusing for a greater distance will encounter a greater range of internal magnetic field inhomogeneities, $\Delta B_0(\mathbf{r})$, we expect the off-diagonal of the spectrum to grow in intensity with increasing displacement. In the top row of Fig. 6, we see that for a Z-displacement of 0 μm, there is a narrow off-diagonal. Of course, zero Z displacement does not mean that a spin-bearing molecule has not changed its local field during τ_m. The possibility remains that that some molecules will have diffused to a different field in the transverse (X,Y) displacement plane during Δ, but remained at or returned to their initial Z-position at the end of the diffusion measurement. This will result in some broadening along the off-diagonal even at 0 μm Z-displacement. Increasing τ_m (and hence Δ) makes such broadening even more pronounced as X and Y displacements grow.

To quantify the off-diagonal intensity for each τ_m and Z, we average together two points on either side of the maximum of the off-diagonal slice. These two points are chosen to be the equivalent of a fraction of the full-width-half-maximum (FWHM) of the 1D inhomogeneous spectrum. In this paper, we will look at two different widths, 0.8 FWHM and 1.0 FWHM, the equivalent of 4.3 kHz and 5.2 kHz. This choice is consistent with the compromise between the signal to noise ratio and the sensitivity to exchange as found in reference [9]. The average intensities at these offsets are plotted in Fig. 7a and b as a function of both τ_m and Z, referred to as $I(Z,\tau_m)$.

Mean normalized intensities increase as both τ_m and Z increase. Off-diagonal line broadening occurs because water molecules, whose spectra were acquired during τ_1 evolution encoding (a total period of up to 3.3 ms) are diffusing through inhomogeneous fields to a new local field value at the time of acquisition (which occurs over 6.4 ms). For the purpose of the present analysis we ignore any motional averaging spectral effects which may result from the finite evolution and acquisition times, since these are generally lower than the τ_m values used in this work. Of course, we expect an increase of off-diagonal intensity with increasing Z since the increase in positional displacement increases the possibility of a water molecule having encountered a different local field. For increasing τ_m, both Z and X, Y displacements contribute, further increasing the likelihood of an altered local field, and thus increasing off-diagonal intensity, $I(Z,\tau_m)$.

The simulated propagator-resolved 2D spectra are calculated by including only those particles which have diffused a designated Z-displacement within the 7.5 μm mesh size of our observation cube. The bottom row of Fig. 6 shows the calculated simulated spectra for a τ_m of 160 ms, and Z of 0 μm, 25 μm, and 45 μm. Also shown, in Fig. 7c and d, are the off-diagonal $I(Z,\tau_m)$ data obtained from the simulation at 0.8 FWHM offset and 1.0 FWHM offset. The addition of displacement information allows us to develop a theory incorporating both mixing time and displacement, rather than extracting exchange times by simple single or double exponential fitting, as in the previous method.

4. Theory

We assume that the mean intensity, $I(Z,\tau_m)$, of the off diagonal grows as molecules diffuse to the new local fields. We define, for convenience, a soft well given by $(1-\exp(-R^2/2l_c^2))$, where l_c is a characteristic length. This function represents the conditional probability of a molecule changing its local field so as to contribute to the off-diagonal intensity. It is zero for $R=0$ and 1 as $R\to\infty$ as required. In the Z-resolved experiment, R^2 is the total distance a molecule has diffused such that it ends on a plane of fixed displacement, Z, along the gradient direction, Z. In other words, $R^2 = Z^2 + r^2$ where r is the distance traveled transverse to the magnetic field gradient. Given an *a priori* knowledge of Z at any time τ_m, $I(Z,\tau_m)$ is given by

$$\begin{aligned} I(Z,\tau_m) &\propto \int_0^\infty 2\pi r dr (4\pi D_{eff}\tau_m)^{-1} \\ &\quad\times \exp\left(-\frac{r^2}{4D_{eff}\tau_m}\right)\left(1-\exp\left(-\frac{Z^2+r^2}{2l_c^2}\right)\right) \\ &= const^*\left(1-\frac{2l_c^2}{2l_c^2+4D_{eff}\tau_m}\exp\left(-\frac{Z^2}{2l_c^2}\right)\right) \end{aligned} \tag{4}$$

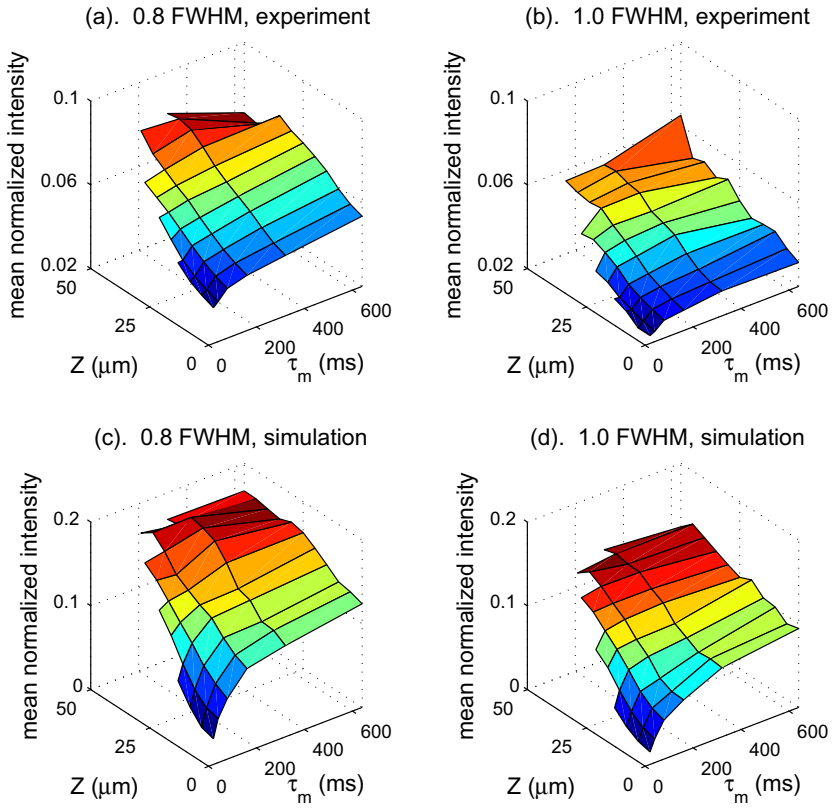

Fig. 7. $I(Z,\tau_m)$ for a τ_m of 160 ms and at different displacements Z. The spectra are normalized to a common total intensity in order to make a visual comparison. (a) For experimental data at 0.8 FWHM. (b) For experimental data at 1.0 FWHM. (c) For simulated data at 0.8 FWHM. (d) For simulated data at 0.8 FHWM.

Weighting $I(Z,\tau_m)$ by the propagator $P(Z,\tau_m)$ and integrating over Z, we obtain the expected result for the non-spatially resolved experiment,

$$I(\tau_m) = const^* \left(1 - \left[\frac{2l_c^2}{2l_c^2 + 4D_{eff}\tau_m}\right]^{3/2}\right) \tag{5}$$

Interestingly, this function differs considerably from the naïve exponential rise assumed in our earlier work and more closely represents the experimental data, as shown in Fig. 8a, where a fit to l_c yields 20 μm for both FWHMs. We repeat this fit for the simulated data as shown in Fig. 8b and obtain an l_c of 23–25 μm for 0.8 FWHM and 1.0 FWHM, respectively. This characteristic length will give us an idea of distance a molecule needs to travel in order to sample a significant range of local fields.

We should observe that the soft well model which led to Eq. (5) is simplistic and does not accurately represent the complexity of the local field distribution. For example, we can see from Fig. 3 that we have a large change in field in the pore throats, which corresponds to a large local magnetic field gradient. A water molecule does not have to diffuse a large distance to experience a large change in magnetic field and thus a corresponding increase in

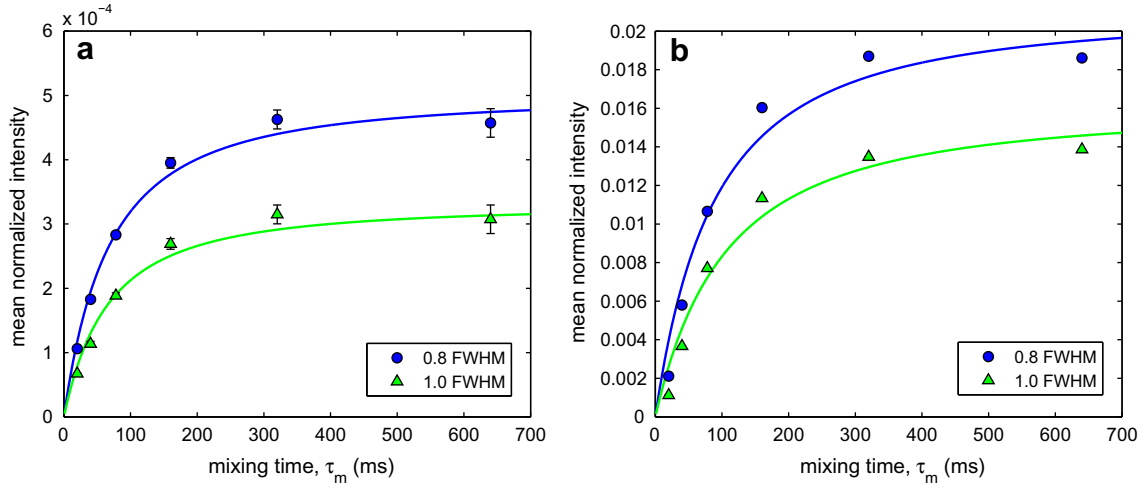

Fig. 8. (a) Calculated off-diagonal intensities from experiment using Eq. (5) with a characteristic length of 20 μm. (b) The same as (a) but with simulated data. Characteristic lengths are 23 and 25 μm for 0.8 FWHM and 1.0 FWHM, respectively.

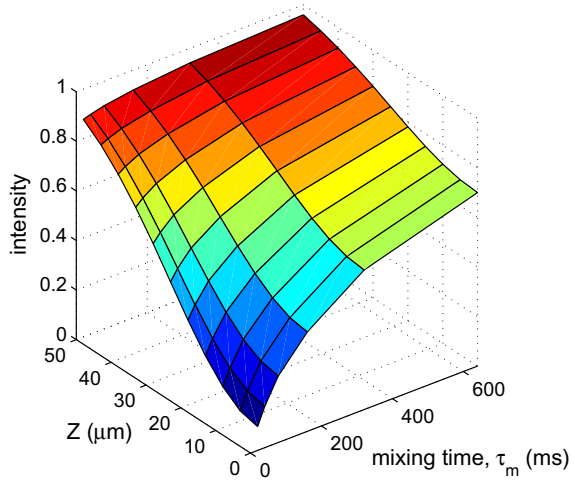

Fig. 9. Calculated off-diagonal intensities using Eq. (4) with a characteristic length of 25 μm.

off-diagonal intensity. This means that the ensemble of molecules will exhibit multiple length scales for field exchange, depending on starting position. Hence it is not surprising that different pulse sequences may return different length scales. However we do find internal consistency within the pulse sequence used here, when we compare fits for propagator-summed and propagator-resolved experiments.

Using the effective diffusion coefficient measured for each τ_m, and our Z-displacements which range from approximately 0 to 50 μm, we plot $I(Z,\tau_m)$ as given by Eq. (4) in Fig. 9. The best representation of our experimental and simulated 2D surfaces shown in Fig. 7 is found by choosing l_c in the range 20–30 μm. An l_c value of around 20 μm is comparable with a typical pore dimension in a 100 μm diameter bead pack. We note that Stapf [19] found correlation lengths of 0.35–0.4 bead diameters for simulated diffusion in a monodisperse bead pack. Audoly et al. [20] suggest that it is the pore dimension which provides the relevant length scale for internal field variations. Finally, we note that the correspondence between l_c values obtained for both the experiment and the simulation found in our study is encouraging, and provides some support for the simple physical concepts used in the analysis of our results.

5. Conclusions

In this paper, we present results of a propagator-resolved field exchange experiment. By adding a displacement dimension to the previous frequency exchange experiment, we are able to separate 2D spectra by both spatial displacement and mixing time rather than just by mixing time alone. We find off-diagonal intensities increase with increasing Z and τ_m which is to be expected. The results of a simulation also produce similar results. A simple theory based on a characteristic length over which significant changes in local field occur, gives good agreement with both experiment and simulations. The new insight here concerns the use of a spatio-temporal approach which has the advantage of yielding a characteristic length from an exchange experiment in a more natural manner.

References

[1] E.O. Stejskal, J.E. Tanner, Spin diffusion measurements: spin echoes in the presence of a time-dependent field gradient, J. Chem. Phys. 42 (1) (1965) 288–292.
[2] R.L. Kleinberg, M.A. Horsfield, Transverse relaxation processes in porous sedimentary rock, J. Magn. Reson. 88 (1990) 9–19.
[3] P.J. McDonald, J.-P. Korb, J. Mitchell, L. Monteilhet, Surface relaxation and chemical exchange in hydrating cement pastes: a two-dimensional NMR relaxation study, Phys. Rev. E 72 (2005) 011409.
[4] K.E. Washburn, P.T. Callaghan, Tracking pore to pore exchange using relaxation exchange spectroscopy, Phys. Rev. Lett. 97 (17) (2006) 175502/1–175502/4.
[5] L. Venkataramanan, Y.Q. Song, M.D. Hurlimann, Solving Fredholm integrals of the first kind with tensor product structure in 2 and 2.5 dimensions, IEEE Trans. Signal Process. 50 (5) (2002) 1017–1026.
[6] S. Godefroy, P.T. Callaghan, 2d relaxation/diffusion correlations in porous media, Magn. Reson. Imag. 21 (3–4) (2003) 381–383.
[7] Y.-Q. Song, S. Ryu, P.N. Sen, Determining multiple length scales in rocks, Nature 406 (6792) (2000) 178–181.
[8] R.R. Ernst, G. Bodenhausen, A. Wokaun, Principles of Nuclear Magnetic Resonance in One and Two Dimensions, Oxford University Press, 2003.
[9] L.M. Burcaw, P.T. Callaghan, Observation of molecular migration in porous media using 2d exchange spectroscopy in the inhomogeneous magnetic field, J. Magn. Reson. 198 (2009) 167–173.
[10] J. Jeener, B.H. Meier, P. Bachmann, R.R. Ernst, Investigation of exchange processes by two-dimensional NMR spectroscopy, J. Chem. Phys. 71 (1979) 4546–4553.
[11] R.J. Brown, Distribution of fields from randomly placed dipoles – free-precession signal decay as result of magnetic grains, Phys. Rev. 121 (5) (1961) 1379–1382.
[12] L.E. Drain, Broadening of magnetic resonance lines due to field inhomogeneities in powdered samples, Proc. Phys. Soc. Lond. 80 (518) (1962) 1380.
[13] K.E. Washburn, P.T. Callaghan, Propagator resolved transverse relaxation exchange spectroscopy, J. Magn. Reson. 186 (2) (2007) 337–340.
[14] K.E. Washburn, C.H. Arns, P.T. Callaghan, Pore characterization through propagator-resolved transverse relaxation exchange, Phys. Rev. E 186 (2008) 051203.
[15] R.M. Cotts, M.J.R. Hoch, T. Sun, J.T. Markert, Pulsed field gradient stimulated echo methods for improved NMR diffusion measurements in heterogeneous systems, J. Magn. Reson. 83 (1989) 252–266.
[16] M.W. Hunter, A.N. Jackson, P.T. Callaghan, NMR measurement and lattice-Boltzman simulation of the non-local dispersion tensor, Phys. Fluids 22 (2010) 027101.
[17] A. Coy, P.T. Callaghan, Pulsed gradient spin-echo NMR diffusive diffraction experiments on water surrounding close-packed polymer spheres, J. Colloid Interface Sci. 168 (1994) 373–379.
[18] P.N. Sen, L.M. Schwartz, P.P. Mitra, B.I. Halperin, Surface relaxation and the long-time diffusion coefficient in porous media: periodic geometries, Phys. Rev. B 49 (1994) 215–225.
[19] S. Stapf, NMR investigations of correlations between longitudinal and transverse displacements in flow through random structured media, Chem. Phys. 284 (2002) 369–388.
[20] B. Audoly, P.N. Sen, S. Ryu, Y.-Q. Song, Correlation functions for inhomogeneous magnetic field in random media with application to a dense random pack of spheres, J. Magn. Reson. 164 (2003) 154–159.